Development 140, 2847 (2013) doi:10.1242/dev.098830

Programmed reduction of ABC transporter activity in sea urchin germline progenitors

Joseph P. Campanale and Amro Hamdoun

There was an error published in *Development* **139**, 783-792.

The left and right designations were inadvertently switched in Fig. 7. In Fig. 7C, the *y*-axis should refer to the right, not left, coelomic pouch. The corrected Fig. 7 legend is shown below. In addition, on p. 789 (lines 46 and 50) and p. 790 (line 58), where a 3/5 left-right distribution is referred to, the correct designation should be 5/3 left-right.

The authors apologise to readers for this mistake.

Fig. 7. Inhibiting ABC transporter activity in the whole sea urchin embryos causes small micromeres to become more randomly segregated. (**A**,**B**) MIPs of embryos injected with mCherry-SpVasa mRNA to localize the small micromeres in red, and treated with 0.3% DMSO, 5 μM MK571 or 3 μM PSC833 in (A) representative embryos and (B) coelomic pouches. Images combined with DIC channel in 96- to 110-hour-old plutei. White arrowheads indicate the right coelomic pouch. Numbers in B indicate the number of Vasa-positive cells counted in each right coelomic pouch. (**C**) Number and percent of small micromeres in the right coelomic pouch of mCherry-Sp-Vasa overexpressing embryos treated with DMSO (*n*=45), MK571 (*n*=38) or PSC833 (*n*=44). (**D**) Average percent (±s.e.m., ≥4 embryos measured per batch) of embryos with right/left coelomic pouch distributions outside of either 3/5 or 4/4 (right pouch/left pouch) from eight batches for the DMSO treatment, six batches for MK571 and seven batches for PSC833. Asterisk indicates values significantly different from the DMSO control (ANOVA, $P \leq 0.5$ with square root transformed values). Scale bars: 25 □m in A; 10 μm in B.

Development 139, 783-792 (2012) doi:10.1242/dev.076752

Programmed reduction of ABC transporter activity in sea urchin germline progenitors

Joseph P. Campanale and Amro Hamdoun*

SUMMARY

ATP-binding cassette (ABC) transporters protect embryos and stem cells from mutagens and pump morphogens that control cell fate and migration. In this study, we measured dynamics of ABC transporter activity during formation of sea urchin embryonic cells necessary for the production of gametes, termed the small micromeres. Unexpectedly, we found small micromeres accumulate 2.32 times more of the ABC transporter substrates calcein-AM, CellTrace RedOrange, BoDipy-verapamil and BoDipy-vinblastine, than any other cell in the embryo, indicating a reduction in multidrug efflux activity. The reduction in small micromere ABC transporter activity is mediated by a pulse of endocytosis occurring 20-60 minutes after the appearance of the micromeres – the precursors of the small micromeres. Treating embryos with phenylarsine oxide, an inhibitor of endocytosis, prevents the reduction of transporter activity. Tetramethylrhodamine dextran and cholera toxin B uptake experiments indicate that micromeres have higher rates of bulk and raft-associated membrane endocytosis during the window of transporter downregulation. We hypothesized that this loss of efflux transport could be required for the detection of developmental signaling molecules such as germ cell chemoattractants. Consistent with this hypothesis, we found that the inhibition of ABCB and ABCC-types of efflux transporters disrupts the ordered distribution of small micromeres to the left and right coelomic pouches. These results point to tradeoffs between signaling and the protective functions of the transporters.

KEY WORDS: Small micromeres, ABC transporters, Germline, Multidrug, Sea urchin

INTRODUCTION

Plasma membranes (PMs) function to control the flow of molecules between cells and their environment. ATP-binding cassette (ABC) transporters are PM proteins found in all cells that provide protection by exporting toxins (Dean et al., 2001; Deeley et al., 2006) and control cell differentiation by exporting morphogens (Fletcher et al., 2010). It is generally presumed that multidrug type ABC transporters, including ABCB-type (permeability glycoprotein or P-gps), ABCC-type (multidrug resistance proteins or MRPs) and ABCG-type (breast cancer resistance protein or BCRP) are abundant in embryos and stem cells to protect them from mutagens.

Previous studies indicate that ABCB, ABCC and ABCG efflux activities control cellular differentiation during development. For example, cell differentiation in *Dictyostelium* is regulated by the ABC transporters TagA, RhT and TagCm (Anjard et al., 1998; Good and Kuspa, 2000; Good et al., 2003), and plants use the transporters to create gradients of auxin (Geisler and Murphy, 2006; Christie et al., 2011). In animal embryos, dauer larva formation in *C. elegans* is controlled by ABCC transporters (Yabe et al., 2005) and in *Drosophila*, ABCB-transporters efflux prenylated peptides from somatic mesoderm to attract germ cells (Ricardo and Lehmann, 2009). Relatively little is known about the pattern of ABC transporter expression in deuterostome embryos, or how their roles in protection and signaling are balanced during development.

Marine Biology Research Division, Scripps Institution of Oceanography, University of California San Diego, 9500 Gilman Drive, La Jolla, CA 92093-0202, USA.

*Author for correspondence (ahamdoun@ucsd.edu)

Accepted 14 December 2011

Previously, we found cleavage stage sea urchin embryos have two multidrug efflux activities mediated by ABCB- and ABCC-type transporters (Hamdoun et al., 2004). Here, we investigated the dynamics of ABC transporter activity during the 4th-6th cell divisions in sea urchins, which correspond to the onset of major cell specification events in this embryo. The 4th cleavage division is asymmetric, producing four macromeres and four micromeres (Horstadius, 1950; McClay, 2011). At the 5th cleavage, micromeres divide to produce four large micromeres and four small micromeres. The four small micromeres divide only once more prior to gastrulation to form eight cells, which migrate to the coelomic pouches formed from mesenchymal pockets on either side of the advancing archenteron (Pehrson and Cohen, 1986; Tanaka and Dan, 1990; Cameron et al., 1991). Small micromeres in the left coelomic pouch proliferate throughout larval development to become the adult rudiment (Juliano et al., 2010). They express canonical germline genes, including *vasa*, *nanos* and *piwi* (Juliano et al., 2006), and are presumed to be progenitors of the germline (Yajima and Wessel, 2010), because their ablation leads to adults that lack gametes.

Unexpectedly, we find that ABC transporter activity is downregulated in the small micromeres, despite their apparent significance to formation of the germline. The downregulation occurs during the 5th cleavage as the micromeres are producing the small and large micromere membranes. Large micromere transport activity eventually returns to levels observed in other blastomeres, but remains reduced in small micromeres. The reduction of multidrug efflux is maintained throughout early development and persists in small micromeres of blastulae. We found the downregulation of multidrug efflux is coincident with a pulse of endocytic activity that peaks after micromeres appear, and results in retrieval of the apical membrane marker ganglioside M1 (GM1). Finally, we found that growing embryos in the presence of ABC transporter inhibitors perturbed the pattern of small micromere

segregation to the coelomic pouches, suggesting that this reorganization of the small micromere PM promotes their ordered distribution.

MATERIALS AND METHODS

Echinoderm collection, gamete gathering and embryo culture

Adult *Strongylocentrotus purpuratus*, *Lytechinus pictus* and *Dendraster excentricus* were collected in La Jolla (CA, USA) and held between 10°C and 12°C in flow-through seawater aquaria. Animals were spawned by intracoelomic injection of 0.55 M KCl. For all experiments, eggs from females were collected in natural seawater (NSW) and washed twice with 0.22 μm filtered seawater (FSW). Eggs were diluted to either a 1% (v/v) suspension, or to 500 eggs/ml in FSW and fertilized in a final sperm dilution of 1:250,000.

Reagents, ABC transporter inhibitors and substrates

Calcein-acetoxymethyl ester (CAM) was from Biotium (Hayward, CA, USA). Bo-dipy-FL Verapamil (BFLVp), Bo-dipy-FL Vinblastine (BFLVb), Hoechst 33342, tetramethylrhodamine dextran (RhoDex, 10,000 MW), cholera toxin B (CTB) and CellTrace RedOrange calcein-AM (CTRO) were from Invitrogen (Carlsbad, CA, USA). MK571, actinomycin D (ActD), brefeldin A (BfA), cadmium chloride, phenylarsine oxide (PAO) and wortmannin (Wort) were from Sigma-Aldrich (St Louis, MO, USA). PSC833 was a gift from Novartis (Basel, Switzerland). All substrates and inhibitors were either dissolved in dimethyl sulfoxide (DMSO) or FSW. Final DMSO concentrations did not exceed 0.5% and solvent controls were used in all experiments.

The cDNA encoding *Sp-vasa* was a gift from Zackary Swartz and Gary Wessel (Gustafson and Wessel, 2010; Voronina et al., 2008). *Sp-vasa* was amplified by PCR and cloned into a PCS2+ vector to yield an N-terminal mCherry fusion. Capped mRNA was synthesized in vitro using a SP6 mMessage mMachine kit (Ambion, Austin, TX, USA), precipitated in lithium chloride and resuspended in deionized H_2O. Capped mRNA was diluted to 1.0 mg/ml and injected at 2-5% of egg volume (Lepage and Gache, 2004).

Quantification of CAM efflux activity using confocal microscopy

Calcein-AM (CAM) is a neutral, non-fluorescent, PM permeable substrate of ABCB/P-gp and ABCC/MRP-type ABC transporters of echinoderm eggs and embryos (Hamdoun et al., 2004; Roepke et al., 2006). Active transporters efflux CAM, whereas cells with reduced or inactive transporters accumulate CAM, which is cleaved by esterases to fluorescent calcein (Essodaigui et al., 1998). Embryos were incubated in CAM and intracellular calcein accumulation was measured using a Zeiss LSM-700 laser scanning confocal microscope (Jena, Germany) equipped with a Zeiss Plan APOChromat 20× air objective (numerical aperture, 0.8). The Zen software suite (Zeiss, revision 5.5) was used to capture images.

To measure calcein accumulation rates in micromeres and small micromeres, compared with the rest of the embryo (ROE), sea urchins were incubated in 250 nM CAM starting at 120 minutes post-fertilization in protamine sulfate-coated Delta-T tissue culture dishes, covered by a coverglass lid to prevent evaporation (Bioptechs, Butler, PA, USA). Approximately 500 embryos in 1 ml were placed into each dish, and kept chilled to 14-15°C using a cooled stage. Fourteen 2.79 μm *z*-sections were taken through 36 μm of the embryos, every 4 minutes for the next 8 hours. Calcein was imaged using a 10 mW 488 nm solid state laser at 0.9% (27 μW) at the sample plane.

Maximum intensity projections (MIPs) were used to quantify the intracellular fluorescence of small micromeres, large micromeres and their descendants, and the rest of the embryo using Volocity (version 5.2, Perkin-Elmer, Waltham, MA, USA). Micrographs were prepared using ImageJ (National Institutes of Health, Bethesda, MD, USA) and Adobe Photoshop CS2.

Identification of transport activities downregulated in small micromeres

Embryos were exposed to 250 nM CAM and inhibitors of either ABCB-transporters (P-gp) or ABCC-transporters (MRP), PSC833 or MK571 beginning at 15 hours post-fertilization. Calcein accumulation was measured at 16.5 hours post-fertilization as described above. Intracellular fluorescence was quantified using ImageJ and calcein concentration was calculated from a standard curve of known calcein solutions.

Inhibition of cellular processes involved in the downregulation of efflux

To identify the cellular mechanism(s) responsible for downregulation of transport, we treated embryos with inhibitors of several cellular processes. To inhibit transcription and anterograde Golgi traffic, embryos were incubated in ActD and BfA starting 30 minutes post-fertilization. To inhibit endocytosis or exocytosis, embryos were treated with cadmium chloride, PAO or wortmannin when 50% of the batch was 16 cells. With all inhibitors, embryos were incubated in CAM 10 minutes after 50% of each batch reached 16 cells and calcein accumulation in micromeres and the ROE was measured 80 minutes later, as described above.

Quantification of fluid phase and GM1 endocytosis

Tetramethylrhodamine dextran experiments were modified from those of Whalley et al. (Whalley et al., 1995) and cholera toxin B experiments were modified from those of Alford et al. (Alford et al., 2009). Eggs were washed as described above, but de-jellied in acid FSW (pH 4.9) for 10 minutes, washed with FSW and fertilized in the presence of 4 mM para-amino benzoic acid (PABA), which inhibits hardening of the fertilization envelope (Wessel and Vacquier, 2004). Envelopes were removed by passage through a 61 μm nitex mesh and cultured at 15°C.

Sixteen-cell stage embryos were treated with either 100 μM rhodamine dextran (10,000 MW) or 5 μg/ml cholera toxin B (CTB) for 20 minutes. Embryos were washed twice with five volumes of ice-cold FSW and fixed on ice for 2 hours in fix solution (0.3% glutaraldehyde, 3% paraformaldehyde, 70% FSW), transferred to PBS and imaged by confocal using a Zeiss C-APOChromat 40× water objective (numerical aperture: 1.1). Embryos exposed to cholera toxin B were rinsed once in hyaline extraction medium (McClay and Fink, 1982) for 5 minutes before incubation with CTB.

Quantification of endosomes labeled with either rhodamine dextran or CTB was carried out using Volocity (Perkin Elmer, San Jose, CA, USA). MIPs were manually thresholded to ensure all of the endosomes were identified (supplementary material Fig. S1). The diameter, volume and surface area of all of the endosomes in each cell was then measured automatically.

Small micromere migration assays

One-cell embryos were injected with the mRNA encoding the *Sp-vasa* construct described above. At 24 hours post-fertilization (HPF), embryos were transferred to 10 ml culture dishes containing either 0.3% DMSO, 5 μM MK571 or 3 μM PSC833 for another 72-85 hours. Embryos were placed on cover slips coated with protamine sulfate (1.0%) and imaged by confocal microscopy using the 20× air objective described above. The numbers of small micromeres were manually tallied from embryos with a total of eight small micromeres that had completed migration to either the left or the right coelomic pouch. Only embryos oriented in such a way that both coelomic pouches were visible were counted. MIPs were prepared using ImageJ.

Statistics

All statistics were analyzed using JMP8.0 (Cary, NC, USA). In all cases, an ANOVA ($\alpha \leq 0.05$) with either Tukey-Kramer or Steel-Dwass tests were used for post-hoc multiple comparisons to analyze for statistical differences between treatments among embryos from multiple females. The number of batches and embryos used for each experiment are given in each figure legend.

RESULTS

Transport activity changes in sea urchin small micromeres

Calcein-AM (CAM) is a non-fluorescent substrate of ABCB- and ABCC-efflux transporters. If these transporters are active, CAM is effluxed from cells. If these transporters are inactive, CAM enters

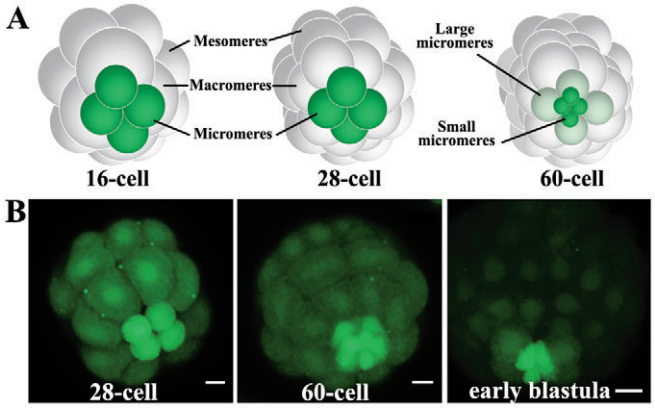

Fig. 1. Sea urchin micromeres and small micromeres accumulate calcein from their appearance through blastulation. (**A**) Schematic diagrams of the 16-, 28- and 60-cell stage embryos. Each stage is shown from a vegetal view. At the 16-cell stage, the micromeres are green. All cells in the embryo, except the micromeres, progress through one cell cycle to produce the 28-cell embryo. At the 60-cell stage, the micromeres have divided into the large micromeres and the small micromeres. (**B**) Maximum intensity projections (MIPs) of *S. purpuratus* embryos showing two developmental switches in calcein accumulation; first, increased in the micromeres (Mics), but not the macromeres (Macs) or the mesomeres (Mes) of the 28-cell stage embryo, and later increased in the large micromeres (Lmic) and small micromeres of the 60-cell embryo; and second, decreased to levels observed in the Mac and Mes for the Lmics in the early blastula. Scale bars: 10 μm.

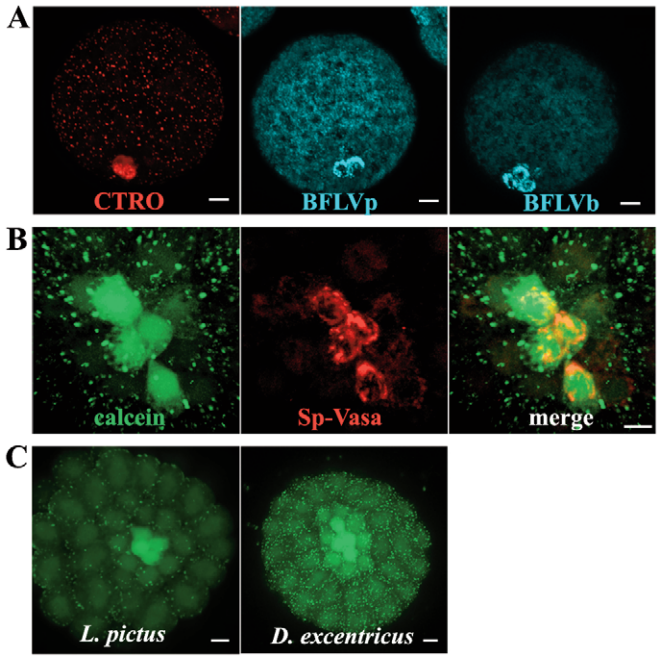

Fig. 2. Small micromeres from sea urchin and sand dollar blastulae accumulate multiple ABC transporter substrates. (**A**) MIPs of blastulae showing small micromeres accumulate more CTRO, BFLVp and BFLVb. (**B**) Vegetal view of a blastula overexpressing Sp-vasa-mCherry fusion protein. Small micromeres are labeled with intracellular calcein in green and Sp-vasa in red. (**C**) MIPs of embryos from *L. pictus* and *D. excentricus* treated with CAM at the 60-cell stage. Scale bars: 10 μm in A,C; 3 μm in B.

the cell and is cleaved by esterases to yield calcein, which is fluorescent and membrane impermeant. Using this substrate, we surveyed transporter activity in embryos from the purple sea urchin *Strongylocentrotus purpuratus*.

In the 16-cell sea urchin embryo, asymmetric cleavage results in the production of three different cell populations each named based on their relative size. These are: (1) four micromeres at the vegetal pole; (2) four macromeres positioned on the vegetal half of the embryo; and (3) eight mesomeres in the animal half of the embryo (Fig. 1A). Subsequently, the macromeres and the mesomeres undergo one cell division to produce a 28-cell embryo before all cells in the embryo divide to produce a 60-cell embryo (Fig. 1A). At this time, the micromeres divide to produce small micromeres and large micromeres (Fig. 1A).

We observed that after the 4th cleavage (i.e. 16-cell stage), the micromeres accumulated more calcein (Fig. 1B) than the rest of the embryo (ROE). Exposure to CAM during the 5th cleavage (i.e. 16-28-cell stage) resulted in both the large and small micromeres accumulating high levels of calcein (Fig. 1B). However, if CAM treatment was postponed until after the small micromeres appeared (60-cell, Fig. 1B), only the small micromeres accumulated calcein. These results indicate two switches in efflux activity between the 4th and 6th cleavages. The first switch results in reduced efflux activity in the micromeres and small micromeres. The second switch restores efflux activity in the large micromeres.

As small micromeres are smaller than other cells in the embryo, we asked whether this phenomenon could be attributed to increases in surface to volume ratios. To test this possibility, we exposed blastulae (15-17 hours post-fertilization) to CAM and three other fluorescent ABC transporter substrates. In blastulae, small micromeres have a surface-to-volume ratio of roughly 0.36 μm^{-1} (diameter of 8 μm and a height of 17.5 μm), similar to the surface-to-volume ratio of the cells in the rest of the embryo 0.32 μm^{-1} (diameter of 9.5 μm and a height of 17.5 μm). The three additional substrates included one requiring esterase activity, CellTrace calcein red-orange AM (CTRO) and two substrates that do not require esterase activity – Bodipy verapamil (BFLVp) and Bodipy vinblastine (BFLVb). We found that all three of these compounds accumulated at higher levels in four cells at the vegetal pole of the embryos (Fig. 2A).

To determine whether the cells labeled in blastulae were indeed the small micromeres, we injected mRNA encoding a red fluorescent protein fusion of Sp-Vasa, which selectively accumulates in the small micromeres (Gustafson and Wessel, 2010; Voronina et al., 2008). The calcein and fluorescent Vasa protein colocalized to the same four cells, confirming that they were the small micromeres (Fig. 2B). Collectively, these experiments eliminated the possibility that differences in surface area-to-volume ratios between the small micromeres and other cells in the embryo at the 60-cell stage, or esterase distribution in these cells are responsible for the increased accumulation of ABC transporter substrates in the small micromeres.

Finally, to determine whether this phenomenon is exclusive to *S. purpuratus*, we tested whether small micromeres of other echinoid species also have reduced calcein efflux activity. We found small micromeres of the sea urchin *Lytechinus pictus* and the sand dollar *Dendraster excentricus* accumulated calcein (Fig. 2C), indicating that this phenomenon has been conserved for more than 250 million years (Smith et al., 2006).

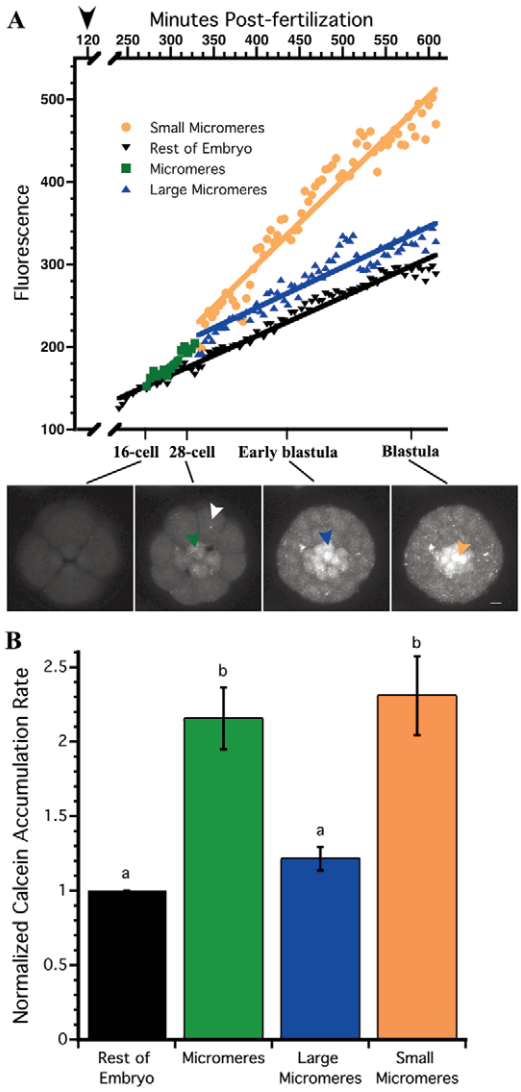

Fig. 3. The rate of calcein accumulation is faster in micromeres and small micromeres than in large micromeres and the rest of the embryo. (**A**) MIPs of *S. purpuratus* embryos accumulating calcein throughout early development. White, green, blue and orange arrowheads indicate each region of interest graphed for the rest of the embryo, micromeres, large micromeres and small micromeres, respectively. Black arrowhead on the graph indicates the start of CAM incubation. Scale bar: 10 μm. (**B**) Rates of calcein accumulation observed for each region of interest and normalized to basal accumulation of the rest of the embryo. Bars are the average of seven embryos from three females (±s.e.m.) and bars sharing the same letter are not significantly different from one another (ANOVA, $P \leq 0.5$), white bars with different letters are significantly different ($P \leq 0.05$).

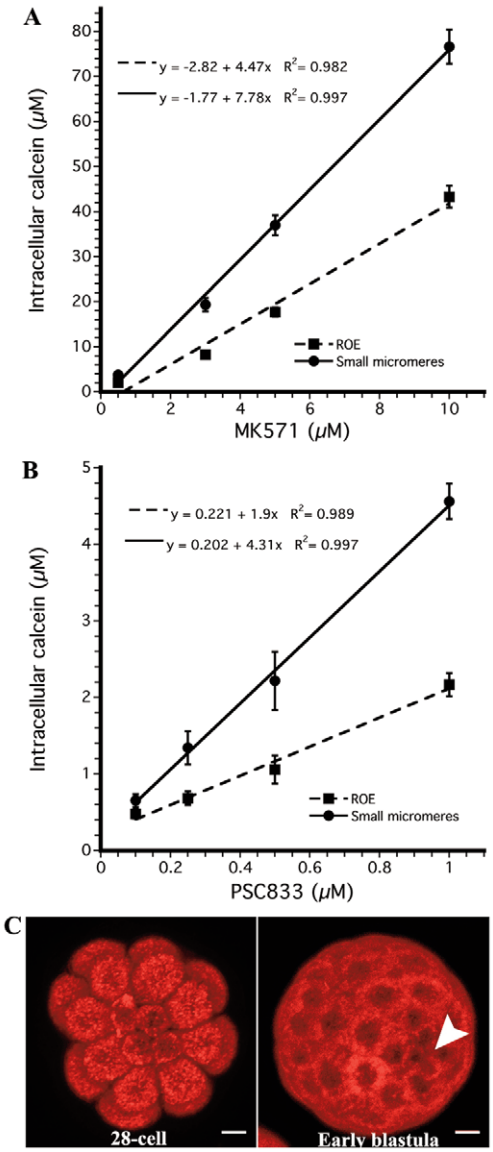

Fig. 4. ABCB- and ABCC-type transport activity is downregulated in the small micromeres. (**A**) Average (±s.e.m.) intracellular calcein concentration for the rest of the sea urchin embryo (dashed line) and small micromeres (solid line) after treatment with MK571, an inhibitor of MRP-efflux transporters [n=5×3 (batches × embryos) measured for each concentration] and (**B**) PSC833, an inhibitor of MDR-efflux transporters (n=4×5). (**C**) MIP of the vegetal view of a 28-cell and 60-cell embryo treated with the fluorescent ABCG2 substrate 1 μM mitoxantrone. Small micromeres are marked by a white arrow. All of the cells in the embryo accumulate the same amount of mitoxantrone. See also supplementary material Fig. S2. Scale bars: 10 μm.

Rates of calcein accumulation in micromeres and small micromeres are higher than those of large micromeres and other blastomeres

To determine the timing of transport activity changes occurring in small micromeres, we measured calcein accumulation rates by 4D confocal microscopy (Fig. 3A; supplementary material Movie 1). Fig. 3A shows maximum intensity projections from a time-lapse video beginning at the four-cell stage and continuing through the early blastula. To measure the differences in efflux activity among cell types, we manually identified regions of interest in each image and measured the accumulation of fluorescent calcein over time (Fig. 3A). Linear regressions were applied to each region to estimate the rate of calcein accumulation in each cell type. The slope for each region was then compared with the basal rate observed in the rest of the embryo (Fig. 3B). The results indicate multidrug efflux activity significantly decreases in the micromeres with a 2.24-fold increase in calcein accumulation rate (P<0.01). After the micromeres divide, the large micromeres return to the same rate observed in the ROE, whereas the small micromeres continue to accumulate calcein at a rate 2.32 times higher than the ROE.

Table 1. Average rate of calcein accumulation in different cells throughout early development

Developmental stage	Approximate time (minutes after fertilization)	Region of embryo	Average accumulation rate (calceins/pl/minute)*
Eight cell	220	Rest of embryo	9397 (±359)
Sixteen cell	270	Micromeres	10,293 (±364)
		Rest of embryo	7261 (±231)
	320	Micromeres	12,292 (±373)
		Rest of embryo	7525 (±241)
Early blastula	520	Small micromeres	12,624 (±1050)
		Large micromeres	7386 (±426)
		Rest of embryo	5756 (±294)

*n=6×≥5 (batches × embryos) ±s.e.m.

To confirm the changes in rate observed by time-lapse analysis, instantaneous calcein accumulation rates were measured from embryos incubated in the dark (i.e. without continuous imaging). The rates of calcein molecules accumulated over time are presented in Table 1. Prior to the appearance of the micromeres, blastomeres of the eight-cell embryo accumulated calcein at a rate of 9397 molecules/pl/minutes [±360 (s.e.m.)]. During the subsequent (i.e. 5th) division, the rate of calcein accumulation in mesomeres and macromeres was 7261 molecules/pl/minutes (±231), whereas the micromere rate was 1.41-fold higher at 10,293 molecules/pl/minutes (±364). After the 60-cell stage, the large micromeres accumulated 7386 molecules/pl/minutes (±426), a rate similar to that measured in the ROE (Fig. 3C), whereas small micromeres accumulated 12,624 molecules/pl/minutes (±1050; Fig. 1A-C), a rate that is 2.19 times higher than the ROE.

Results from both the measurement of calcein accumulation by time-lapse confocal and the instantaneous rate calculations confirm the two developmental switches described in Fig. 1B. An initial reduction of ABC transporter-mediated efflux of calcein occurs early in the micromere cell cycle but this decrease in multidrug efflux activity is maintained only in the small micromere lineage, whereas it returns to normal in the large micromeres.

ABCB- and ABCC-type transporters are downregulated in the small micromeres

Previous work demonstrated that two types of ABC transporter activities are responsible for calcein efflux in sea urchin embryos (Hamdoun et al., 2004). One is pharmacologically similar to ABCB/P-gp-like transport and another is similar to ABCC/MRP transport. To identify which of these two activities is downregulated in the small micromeres, we exposed blastulae to inhibitors of ABCB/P-gp or ABCC/MRP transporters (PSC833 and MK571, respectively), and then measured intracellular calcein accumulation. Both MK571 and PSC833 cause dose-dependent increases in calcein accumulation in small micromeres (Fig. 4A,B). However, because small micromeres continue to show inhibitor-sensitive increases in calcein accumulation, we conclude that transport is downregulated rather than completely inactivated.

As ABCG2-efflux transporters are commonly expressed in stem cells (Bunting, 2002), we considered the possibility that some compensatory ABCG activity could be induced in these cells to counteract for loss of the ABCB/C activity. To test this hypothesis, embryos were incubated in the ABCG2 substrate, mitoxantrone and the intracellular accumulation was measured for the micromeres, small micromeres and the ROE. We did not observe a reduction in mitoxantrone accumulation in either the micromeres or the small micromeres, indicating that they do not upregulate the activity of ABCG2 (Fig. 4C). In addition, 5 μM fumitremorgin C, an ABCG2 inhibitor, does not increase accumulation of mitoxantrone (supplementary material Fig. S2), suggesting that these embryos have little or no ABCG2 activity at this stage.

Inhibition of endocytosis limits downregulation of efflux activity in small micromeres

To identify the general cellular mechanism responsible for downregulation of efflux transport, inhibitors were used to perturb endocytosis, exocytosis, transcription and Golgi-to-PM traffic. 16-cell embryos were exposed to inhibitors and the relative increase in micromere fluorescence was measured after treating embryos with each inhibitor. During this experiment, micromeres of control embryos accumulated 1.58 times more calcein than cells in the ROE (Fig. 5A,B). We expected that if the inhibitor perturbed the downregulation of transport, the relative difference in accumulation between micromeres and the rest of the embryo would diminish.

Micromeres of embryos treated with actinomycin D or brefeldin A accumulated 1.60- and 1.57-fold more calcein than the rest of the embryo, respectively, indicating that changes in efflux activity do not require de novo expression of a protein that increases calcein uptake in the micromeres (Fig. 5A). Instead, as many PM proteins are regulated by their insertion and retrieval from membranes, we hypothesized that changes in efflux transport could be due to changes in the PM concentration of efflux transporters. This could either be due to an increase in endocytic retrieval of transporters or to a decrease in exocytic delivery of recycled transporter protein.

To distinguish between these two mechanisms, we investigated whether inhibitors of exocytosis or endocytosis perturb the downregulation of efflux transport in the micromeres. Micromeres of embryos treated with 100 nM wortmannin, an inhibitor of exocytosis (Martys et al., 1996; Spiro et al., 1996), accumulated 1.54 times more calcein than the ROE (Fig. 5A), indicating that decreased membrane recycling is not responsible for the reduction in transport. Cadmium chloride, an inhibitor of one type of compensatory endocytosis in early sea urchin development (Covian-Nares et al., 2008), had no effect on downregulation of transport (Fig. 5A). By contrast, phenylarsine oxide (PAO), an inhibitor of constitutive endocytosis (Covian-Nares et al., 2008), prevented the downregulation of efflux in the micromeres (Fig. 5A,B). Micromeres of embryos treated with 10 μM PAO accumulated only 1.17-fold more calcein than the ROE when compared with 1.58-fold for controls.

Interestingly, when the addition of PAO was postponed until halfway through the micromere cell cycle (50 minutes post appearance of micromeres), we observed a 1.47-fold increase in intracellular calcein for the micromeres, which was not significantly different from the control embryos (P=0.19). Our results indicate that the endocytic event responsible for downregulation of transport occurs within the first half of the

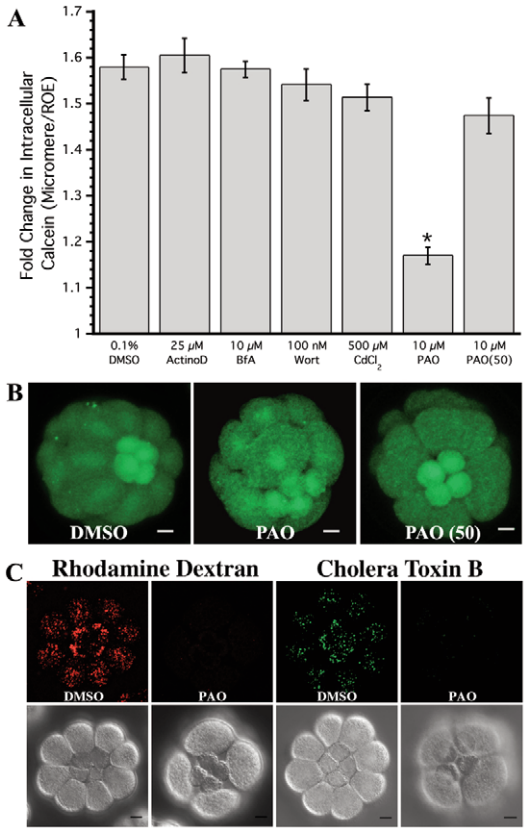

Fig. 5. Inhibiting protein tyrosine phosphatases (PTPs) with PAO stops loss of multidrug efflux transport activity in the micromeres. (**A**) Relative amount of intracellular calcein of the sea urchin micromeres compared with the rest of the embryo [n=3×≥10 (batches × embryos), ±s.e.m.] during treatment with inhibitors of transcription (ActD), Golgi traffic (BfA), endocytosis ($CdCl_2$ and PAO) and exocytosis (Wort). Asterisk indicates values significantly different from control (ANOVA, P≤0.5). Treatment with PAO stops the loss of multidrug efflux, and postponing PAO treatment until 50 minutes after the appearance of the micromeres does not stop the loss of efflux transport [PAO (50)]. (**B**) Representative MIPs of calcein accumulation in embryos treated with DMSO, PAO and PAO (50). (**C**) MIPs showing the cumulative amount of rhodamine dextran and CTB-positive endosomes in micromeres and macromeres for embryos treated with DMSO or PAO for 80 minutes after their appearance. Scale bars: 10 μm.

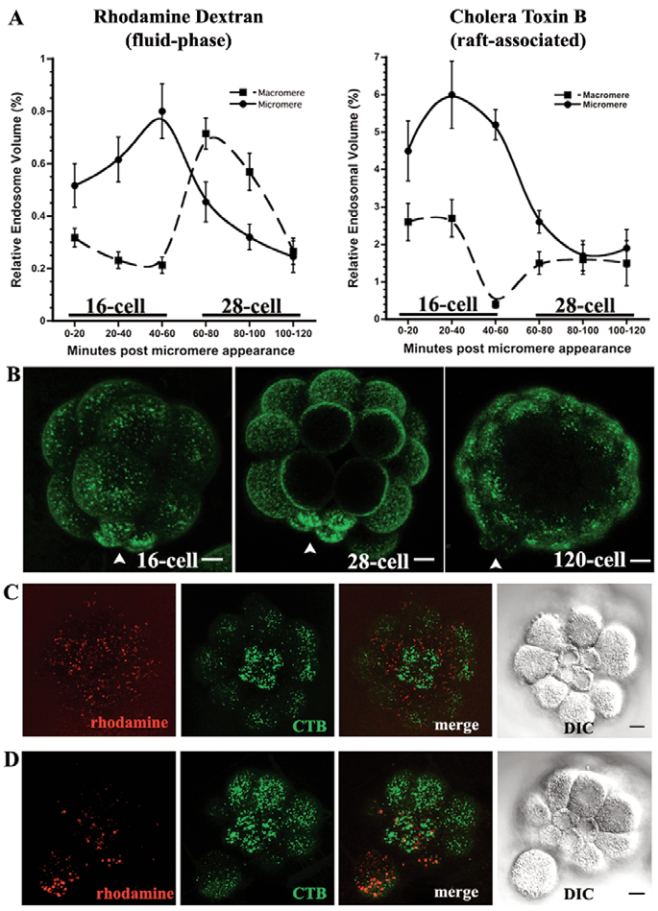

Fig. 6. Fluid-phase and GM1 endocytosis is dynamic throughout the cell cycle, peaking at 40-60 minutes after micromere formation. (**A**) Average relative endosome volume (±s.e.m.) measured in sea urchin micromeres (solid lines) and macromeres (broken lines) using rhodamine dextran [n=3×5×4 (batches × embryos × cells) from each embryo], a marker of fluid-phase endocytosis, and cholera toxin B (n=3×5×4), a marker of GM1 found in lipid rafts. (**B**) MIPs showing endocytosis of CTB in 16-cell, 28-cell and blastulae after a 5-minute labeling period and a 20- to 30-minute uptake interval. Micromeres are labeled with arrowheads. (**C**,**D**) Embryos co-incubated in rhodamine dextran and CTB (C) 20-40 minutes and (D) 40-60 minutes after the appearance of the micromeres showing lack of colocalization of the two markers. See also supplementary material Fig. S1. Scale bars: 10 μm.

micromere cell cycle. In addition, as PAO had no effect on the relative difference in calcein accumulation between micromeres and controls when added after 50 minutes, we conclude that the earlier effects of PAO on relative differences in accumulation are not due to non-specific toxicity.

Endocytic activity in the micromeres

Given that the reduction of transport is observed only in the micromeres, we hypothesized differences in the rate of endocytosis in the micromeres when compared with macromeres correlate with the timing of reduction in efflux activity. To characterize the relative rates of endocytosis in the micromeres, sea urchin embryos were incubated in either 10,000 MW rhodamine dextran or cholera toxin B (CTB) for 20-minute intervals starting immediately after appearance of the micromeres. Rhodamine dextran is a marker for fluid phase endocytosis (Covian-Nares et al., 2008; Whalley et al., 1995; Conner and Wessel, 1998) and CTB binds to gangliosides associated with lipid rafts (Parton, 1994). We quantified endosomes in both micromeres and macromeres for both markers. The number of endosomes and the volume of each endosome were measured from confocal micrographs (Fig. 6A, supplementary material Fig. S1). To account for differences in size between cells, the total volume of all endosomes was normalized to the total cell volume and this fraction was termed the ‘relative endosome volume’ (Fig. 6A).

Consistent with the observation that reduction of multidrug efflux transport activity occurs within 50 minutes of the appearance of the micromeres (Fig. 5A, Table 1), we also found that the endocytic activity peaks in the micromeres between 40-60 minutes for rhodamine dextran and from 20-40 minutes for cholera toxin B (Fig. 6A, supplementary material Fig. S1). For each of these intervals, the total relative volume of rhodamine dextran and CTB endosomes was higher in the micromeres than the macromeres.

From 40-60 minutes after the appearance of the micromeres, an average of 47 rhodamine-positive endosomes were counted per micromere, totaling 0.80% of their volume, whereas the macromeres internalized an average of 87 endosomes during the same window of time, totaling only 0.21% of their volume. Cholera toxin B uptake from 20-40 minutes showed similar trends, with the micromeres internalizing an average of 158 endosomes (6.0% of their volume) while the macromeres endocytosed 570 endosomes totaling only 2.7% of their volume.

Additional evidence indicating enhanced uptake of apical GM1-rich membrane in micromeres came from two observations. First, when we incubated embryos in both CTB and rhodamine dextran during the peak of endocytosis, we found that the two populations of endosomes do not co-localize in the micromeres (Fig. 6C,D) and that dextran localized to fewer, larger endosomes than the CTB, indicating that the two markers are internalized independently. Second, when we incubated embryos in cholera toxin B for 5 minutes at different developmental stages and then washed out unbound CTB, we observed that micromeres of 16- and 28-cell embryos have strong surface labeling, whereas the small micromeres of 60-cell stage embryos had limited CTB labeling (Fig. 5B-D). These results suggest that dividing micromeres have greater retrieval of GM1-rich apical membrane constituents than other cells in the embryo.

Inhibition of efflux transport activity perturbs ordered migration of small micromeres to coelomic pouches

Recent research in *Drosophila* embryos indicates that the protective ABCB transporter Mdr49 (Wu et al., 1991) is also expressed in somatic gonadal precursors and effluxes lipid modified peptides that serve as chemoattractants for migrating germ cells (Ricardo and Lehmann, 2009). Additionally, these authors found that *Drosophila* loss-of-function mutants could be rescued by expression of an orthologous yeast transporter. Based on these results, and on the observation that many aspects of germline specification are conserved among animals, we hypothesized that ABCB and ABCC transporters in sea urchins could guide small micromere migration to the left and right coelomic sacs of the two-armed pluteus larva.

To investigate the potential for multidrug efflux activity to control small micromere migration patterns, we labeled small micromeres with fluorescent Sp-Vasa and grew embryos in transporter inhibitors until the two-armed pluteus stage (96-110 HPF), when the small micromeres have migrated to the coelomic pouches. In 60% of the control embryos, small micromeres segregated in a 3/5 (left coelomic pouch/right coelomic pouch) distribution (Fig. 7A-C), whereas another 32% showed a 4/4 distribution.

By contrast, embryos treated with the transporter inhibitors MK571 or PSC833 showed a reduction in the 3/5 and 4/4 segregation patterns (Fig. 7C) and a significant increase in aberrant segregation (Fig. 7D). We observed significant increases in the frequency of deviant small micromere migration in 60% of MK571-treated embryos and 43% in PSC833-treated embryos (Fig. 7D). Extremely abnormal segregation patterns were observed in both inhibitors, including instances where all eight small micromeres were present in only one coelomic pouch (16% for MK571 and 2% for PSC833, Fig. 7C).

One caveat is that while embryos grown in the presence of PSC833 are morphologically similar to control embryos, treatment with MK571 results in other defects. Embryos grown in 5 μM MK571 complete gastrulation and form both left and right coelomic pouches (Fig. 7A), but these embryos often had severely reduced or, in some cases, a complete lack of skeletal rods. As

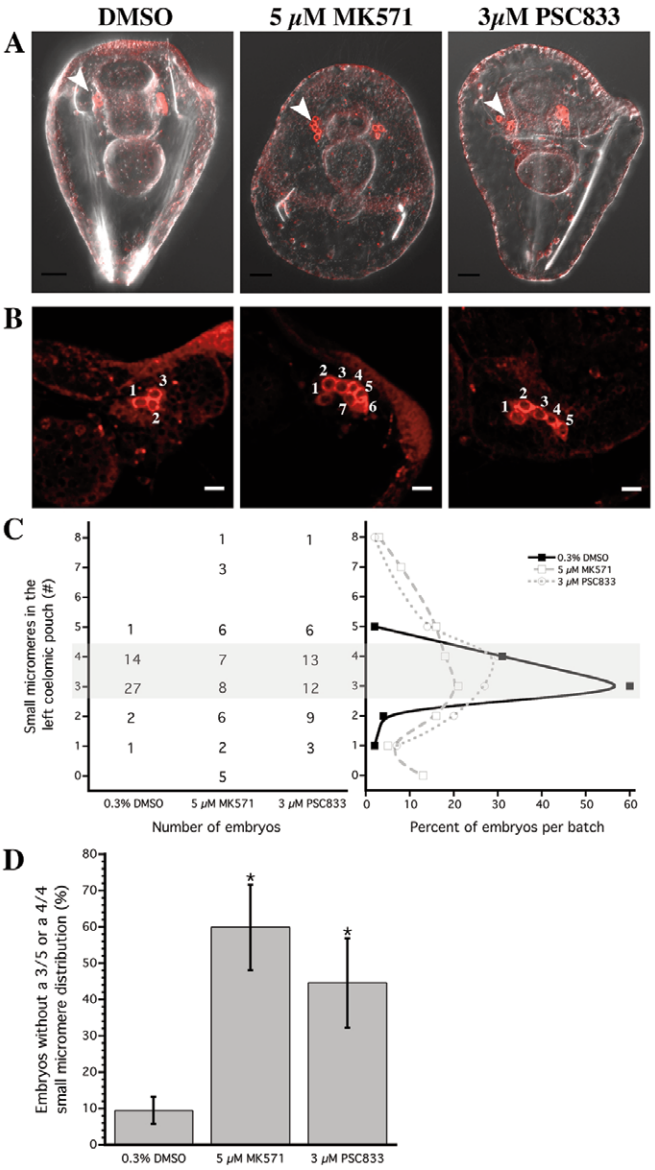

Fig. 7. Inhibiting ABC transporter activity in the whole sea urchin embryos causes small micromeres to become more randomly segregated. (**A**,**B**) MIPs of embryos injected with mCherry-SpVasa mRNA to localize the small micromeres in red, and treated with 0.3% DMSO, 5 μM MK571 or 3 μM PSC833 in (A) representative embryos and (B) coelomic pouches. Images combined with DIC channel in 96- to 110-hour-old plutei. White arrowheads indicate the left coelomic pouch. Numbers in B indicate the number of Vasa-positive cells counted in each left coelomic pouch. (**C**) Number and percent of small micromeres in the left coelomic pouch of mCherry-Sp-Vasa overexpressing embryos treated with DMSO (*n*=45), MK571 (*n*=38) or PSC833 (*n*=44). (**D**) Average percent (±s.e.m., ≥4 embryos measured per batch) of embryos with left/right coelomic pouch distributions outside of either 3/5 or 4/4 (left pouch/right pouch) from eight batches for the DMSO treatment, six batches for MK571 and seven batches for PSC833. Asterisk indicates values significantly different from the DMSO control (ANOVA, $P \leq 0.5$ with square root transformed values). Scale bars: 25 μm in A; 10 μm in B.

MK571 inhibits several different types of ABCC transporters (Zhou et al., 2008) this could either indicate that transport is involved in other processes (such as spiculogenesis) or that MK571 has indirect/non-specific effects. Nonetheless, the observation that both PSC833 and MK571 (which are structurally unrelated) perturb small micromere migration suggests that the left/right allocation of small micromeres to the coelomic pouches involves ABC transporters.

DISCUSSION

Sea urchin small micromeres are specialized cells destined to contribute to formation of gametes. Unexpectedly, we found that these crucial cells have reduced efflux transport activity when compared with other cells in the embryo. This is surprising because robust efflux transport, mediated by ABC transporters, is a canonical feature of multipotent cells under strong selection for protection of their DNA (Dean et al., 2005). In fact, increased expression of efflux transporters is often used to isolate adult and embryonic stem cells termed 'side-population' cells (Zhou et al., 2002; Bunting, 2002; Uchida et al., 2004). Therefore, a priori, we would have expected small micromeres to have higher efflux activity than other cells in the embryo. Given the unexpected nature of this change in small micromere efflux activity, we hypothesized that these changes could be necessary for their specification or migration. Consistent with this hypothesis, we observed that transporter inhibitors interfere with ordered small micromere segregation to coelomic pouches.

One possibility is that the transporter inhibitors perturb segregation by interference with some autonomous property of the small micromeres, perhaps by interference with homing-independent pathways that specify left/right patterning (Duboc et al., 2005). However, as small micromeres already have reduced efflux activity, it seems more likely that inhibitors perturb efflux transporters elsewhere in the embryo. Suppression of efflux transport in small micromeres could be a mechanism for concentrating signals necessary for their later migration to the coelomic pouches of the pluteus larva. This would not be surprising because germline precursors often arise far from the somatic gonad and a common feature of germline cells in many species is chemoattractant-guided migration through mesodermal epithelia to the gonad (Kunwar et al., 2006). In *Danio* (Thorpe et al., 2004) and *Drosophila* (Santos and Lehmann, 2004), the chemoattractants are lipid modified peptides. In *Drosophila* the lipid modified peptides are secreted by an ABCB-transporter (Mdr49) expressed in the somatic gonad, but not in the germ cells, presumably because it would interfere with the reception of the chemoattractant.

Alternatively, it is also possible that small micromere segregation is not robust and is indirectly perturbed by interference with ABC transporter-mediated signaling. Previous studies on the distribution of small micromeres in coelomic pouches show it is variable among echinoderms (Juliano and Wessel, 2009). For example a 5/3 distribution is observed in *Hemicentrotus pulcherrimus* (Fujii et al., 2009; Hara and Katow, 2005), whereas studies using *S. purpuratus* indicate the distribution of small micromeres can be either equal (Cameron et al., 1991) or asymmetric between the left and right pouch (Pehrson and Cohen, 1986; Cameron et al., 1991). However, as we found that that 90% of the control embryos showed either a 3/5 or 4/4 distribution, it seems that segregation is normally tightly regulated. To our knowledge, this is the first study to assess quantitatively these segregation patterns.

The changes we observed in this study occur at the confluence of events that direct vegetal cell fate in sea urchins. This begins with specification of the primary mesenchyme cell fate in micromeres through the selective expression of the transcription factor pmar1 (Oliveri et al., 2003) and the nuclear localization of β-catenin (Logan et al., 1999) in large and small micromeres. There is also selective accumulation of germline determinants, such as vasa (Voronina et al., 2008), only in the small micromeres. It is clear from our study and that of Sparling (Sparling and Kruszewska, 1990) that each of the two lineages produced by micromeres are endowed with different membrane proteins and lipids from the rest of the embryo. Asymmetric partitioning of developmental molecules, including ABC transporters, is likely to be essential for controlling cellular trajectory. For example, budding in yeast results in a short-lived mother cell that retains its original transporters and a long-lived daughter cell that inherits newly synthesized transporters (Eldakak et al., 2010). This mechanism acts like a clock, whereby the newly synthesized transporters reset the mitotic age of the buds.

Our results indicate that endocytosis is a major mechanism for segregation of proteins between the large and small micromere PMs. Previous studies on endocytic activity in earlier stage sea urchin embryos indicate that two independent types of endocytosis are present (Covian-Nares et al., 2008). The first type is inhibited by cadmium chloride and is associated with the retrieval of cortical granule membranes following fertilization. The second type is PAO sensitive and is involved in the retrieval of PM deposited by constitutive exocytosis. Consistent with the previous observation that the cadmium chloride-sensitive mechanism is restricted to retrieval of cortical granule membrane, we found that cadmium chloride had no effect on downregulation of transport. Instead, the PAO-sensitive endocytic pathway, operating in the first half of the 5th division, is responsible for the downregulation of efflux.

A number of different endocytic pathways are inhibited by PAO and these endocytic pathways inhibited could either retrieve the efflux pumps themselves or retrieve a protein or lipid necessary for their activity. At the peak of endocytic activity, micromeres are retrieving twice as much GM1-rich PM than the macromeres. This suggests that the micromeres remove more apical PM than other cells in the embryo, leading to a unique PM composition in the small micromeres. Although the small micromeres are not thought to undergo a bona fide epithelial-mesenchymal transition when they appear, our results and those of other groups, indicate that they may lack or suppress some characters of apical-basal polarity seen earlier in embryogenesis (Alford et al., 2009). For example, Schroeder (Schroeder, 1988) suggested that micromere membranes have fewer microvilli than other cells, when they first appear.

In turn, any changes in cell polarity would probably be coupled to changes in endocytic activity (Shivas et al., 2010). For example, Cdc42, which maintains apical-basal polarity in sea urchin embryos (Alford et al., 2009), can also promote endocytosis. In *Drosophila*, ectodermal inactivation of Cdc42 promotes Rab5-mediated endocytosis of apical proteins (Harris and Tepass, 2010). As Rab5 has been implicated in endocytic retrieval of multidrug transporters (Kim et al., 1997), it is plausible that the endocytic pulses we observed remove ABC transporters from the apical membranes. In addition, as multidrug transporters appear to concentrate in raft microdomains (Klappe et al., 2009), endocytosis could also have a repressive effect on efflux activity by reducing raft lipids.

Beyond providing insight into the mechanisms that regulate the activity and membrane titer of multidrug transporters, the broader significance of these findings are tradeoffs between developmental

and protective functions of poly-specific ABC transporters (Aller et al., 2009; Zhou et al., 2008). ABC efflux transporters in sea urchin embryos play dual protective and developmental roles in the efflux of toxicants and germline precursor specification. Given that transporters have broad substrate specificity, there may be tradeoffs between the protective benefit of high levels of efflux activity and a need for signal reception that limits their activity. In this case the implication of this tradeoff would be that the germline is rendered vulnerable to teratogens as part of development. As key elements of the genetic and biochemical germline specification programs are conserved among animals, these trade-offs could be central to how windows of vulnerability arise from the normally robust programs of differentiation.

Acknowledgements
We thank P. Zerofski for research animals; S. Z. Swartz, G. M. Wessel, K. Whalen and T. Gokirmak for generating the *Sp*-vasa mRNA; L. E. Shipp, V. D. Vacquier, N. D. Holland and D. Epel for valuable discussions; and J. Coffman and K. Uhlinger for assistance and discussions at MDIBL.

Funding
This work was supported by a United States Environmental Protection Agency (EPA) STAR Fellowship [FP-91711601-0 to J.P.C.]; by the National Institutes of Health (NIH) [HD058070 to A.H.]; by a Mount Desert Island Biological Laboratory (MDIBL) New Investigator Award to A.H.; and by support from the Krinsk Research Advancement Initiative to A.H.'s laboratory. Deposited in PMC for release after 12 months.

Competing interests statement
The authors declare no competing financial interests.

Supplementary material
Supplementary material available online at
http://dev.biologists.org/lookup/suppl/doi:10.1242/dev.076752/-/DC1

References

Alford, L. M., Ng, M. M. and Burgess, D. R. (2009). Cell polarity emerges at first cleavage in sea urchin embryos. *Dev. Biol.* **330**, 12-20.
Aller, S. G., Yu, J., Ward, A., Weng, Y., Chittaboina, S., Zhuo, R., Harrell, P. M., Trinh, Y. T., Zhang, Q., Urbatsch, I. L. et al. (2009). Structure of P-glycoprotein reveals a molecular basis for poly-specific drug binding. *Science* **323**, 1718-1722.
Anjard, C., Zeng, C., Loomis, W. F. and Nellen, W. (1998). Signal transduction pathways leading to spore differentiation in *Dictyostelium discoideum*. *Dev. Biol.* **193**, 146-155.
Bunting, K. D. (2002). ABC transporters as phenotypic markers and functional regulators of stem cells. *Stem Cells* **20**, 11-20.
Cameron, R. A., Fraser, S. E., Britten, R. J. and Davidson, E. H. (1991). Macromere cell fates during sea urchin development. *Development* **113**, 1085-1091.
Christie, J. M., Yang, H., Richter, G. L., Sullivan, S., Thomson, C. E., Lin, J., Titapiwatanakun, B., Ennis, M., Kaiserli, E., Lee, O. R. et al. (2011). phot1 inhibition of ABCB19 primes lateral auxin fluxes in the shoot apex required for phototropism. *PLoS Biol*. **9**, e1001076.
Conner, S. and Wessel, G. M. (1998). rab3 mediates cortical granule exocytosis in the sea urchin egg. *Dev. Biol.* **203**, 334-344.
Covian-Nares, J. F., Smith, R. M. and Vogel, S. S. (2008). Two independent forms of endocytosis maintain embryonic cell surface homeostasis during early development. *Dev. Biol.* **316**, 135-148.
Dean, M., Rzhetsky, A. and Allikmets, R. (2001). The human ATP-binding cassette (ABC) transporter superfamily. *Genome Res*. **11**, 1156-1166.
Dean, M., Fojo, T. and Bates, S. (2005). Tumour stem cells and drug resistance. *Nat. Rev. Cancer* **5**, 275-284.
Deeley, R., Westlake, C. and Cole, S. (2006). Transmembrane transport of endo- and xenobiotics by mammalian ATP-binding cassette multidrug resistance proteins. *Physiol. Rev.* **86**, 849-899.
Duboc, V., Röttinger, E., Lapraz, F., Besnardeau, L. and Lepage, T. (2005). Left-right asymmetry in the sea urchin embryo is regulated by nodal signaling on the right side. *Dev. Cell* **9**, 147-158.
Eldakak, A., Rancati, G., Rubinstein, B., Paul, P., Conaway, V. and Li, R. (2010). Asymmetrically inherited multidrug resistance transporters are recessive determinants in cellular replicative ageing. *Nat. Cell Biol.* **12**, 799-805.
Essodaigui, M., Broxterman, H. J. and Garnier-Suillerot, A. (1998). Kinetic analysis of calcein and calcein-acetoxymethylester efflux mediated by the multidrug resistance protein and P-glycoprotein. *Biochemistry* **37**, 2243-2250.
Fletcher, J. I., Haber, M., Henderson, M. J. and Norris, M. D. (2010). ABC transporters in cancer: more than just drug efflux pumps. *Nat. Rev. Cancer* **10**, 147-156.
Fujii, T., Sakamoto, N., Ochiai, H., Fujita, K., Okamitsu, Y., Sumiyoshi, N., Minokawa, T. and Yamamoto, T. (2009). Role of the nanos homolog during sea urchin development. *Dev. Dyn.* **238**, 2511-2521.
Geisler, M. and Murphy, A. (2006). The ABC of auxin transport: The role of p-glycoproteins in plant development. *FEBS Lett*. **580**, 1094-1102.
Good, J. and Kuspa, A. (2000). Evidence that a cell-type-specific efflux pump regulates cell differentiation in *Dictyostelium*. *Dev. Biol.* **220**, 53-61.
Good, J. R., Cabral, M., Sharma, S., Yang, J., Van Driessche, N., Shaw, C. A., Shaulsky, G. and Kuspa, A. (2003). TagA, a putative serine protease/ABC transporter of *Dictyostelium* that is required for cell fate determination at the onset of development. *Development* **130**, 2953-2965.
Gustafson, E. A. and Wessel, G. M. (2010). Exogenous RNA is selectively retained in the small micromeres during sea urchin embryogenesis. *Mol. Reprod. Dev*. **77**, 836.
Hamdoun, A., Cherr, G., Roepke, T. and Epel, D. (2004). Activation of multidrug efflux transporter activity at fertilization in sea urchin embryos (*Strongylocentrotus purpuratus*). *Dev. Biol.* **276**, 452-462.
Hara, Y. and Katow, H. (2005). Exclusive expression of hedgehog in small micromere descendants during early embryogenesis in the sea urchin, Hemicentrotus pulcherrimus. *Gene Expr. Patterns* **5**, 503-510.
Harris, K. P. and Tepass, U. (2010). Cdc42 and vesicle trafficking in polarized cells. *Traffic* **11**, 1272-1279.
Horstadius, S. (1950). The mechanics of sea urchin development. *Annee. Biol*. **26**, 381-398.
Juliano, C., Voronina, E., Stack, C., Aldrich, M., Cameron, A. and Wessel, G. M. (2006). Germ line determinants are not localized early in sea urchin development, but do accumulate in the small micromere lineage. *Dev. Biol.* **300**, 406-415.
Juliano, C. E. and Wessel, G. M. (2009). An evolutionary transition of Vasa regulation in echinoderms. *Evol. Dev*. **11**, 560-573.
Juliano, C., Swartz, S. and Wessel, G. M. (2010). A conserved germline multipotency program. *Development* **137**, 4113-4126.
Kim, H., Barroso, M., Samanta, R., Greenberger, L. and Sztul, E. (1997). Experimentally induced changes in the endocytic traffic of P-glycoprotein alter drug resistance of cancer cells. *Am. J. Physiol*. **273**, C687-C702.
Klappe, K., Hummel, I., Hoekstra, D. and Kok, J. W. (2009). Lipid dependence of ABC transporter localization and function. *Chem. Phys. Lipids* **161**, 57-64.
Kunwar, P. S., Siekhaus, D. E. and Lehmann, R. (2006). In vivo migration: a germ cell perspective. *Annu. Rev. Cell Dev. Biol.* **22**, 237-265.
Lepage, T. and Gache, C. (2004). Expression of exogenous mRNAs to study gene function in the sea urchin embryo. *Methods Cell Biol*. **74**, 677-697.
Logan, C. Y., Miller, J. R., Ferkowicz, M. J. and McClay, D. R. (1999). Nuclear beta-catenin is required to specify vegetal cell fates in the sea urchin embryo. *Development* **126**, 345-357.
Martys, J. L., Wjasow, C., Gangi, D. M., Kielian, M. C., McGraw, T. E. and Backer, J. M. (1996). Wortmannin-sensitive trafficking pathways in Chinese hamster ovary cells. Differential effects on endocytosis and lysosomal sorting. *J. Biol. Chem*. **271**, 10953-10962.
McClay, D. R. (2011). Evolutionary crossroads in developmental biology: sea urchins. *Development* **138**, 2639-2648.
McClay, D. R. and Fink, R. D. (1982). Sea urchin hyalin: appearance and function in development. *Dev. Biol.* **92**, 285-293.
Oliveri, P., Davidson, E. H. and McClay, D. R. (2003). Activation of pmar1 controls specification of micromeres in the sea urchin embryo. *Dev. Biol.* **258**, 32-43.
Parton, R. G. (1994). Ultrastructural localization of gangliosides; GM1 is concentrated in caveolae. *J. Histochem. Cytochem*. **42**, 155-166.
Pehrson, J. and Cohen, L. (1986). The fate of the small micromeres in sea urchin development. *Dev. Biol.* **113**, 522-526.
Ricardo, S. and Lehmann, R. (2009). An ABC transporter controls export of a *Drosophila* germ cell attractant. *Science* **323**, 943-946.
Roepke, T. A., Hamdoun, A. M. and Cherr, G. N. (2006). Increase in multidrug transport activity is associated with oocyte maturation in sea stars. *Dev. Growth Differ*. **48**, 559-573.
Santos, A. and Lehmann, R. (2004). Germ cell specification and migration in *Drosophila* and beyond. *Curr. Biol*. **14**, R578-R589.
Schroeder, T. E. (1988). Contact-independent polarization of the cell surface and cortex of free sea urchin blastomeres. *Dev. Biol.* **125**, 255-264.
Shivas, J. M., Morrison, H. A., Bilder, D. and Skop, A. R. (2010). Polarity and endocytosis: reciprocal regulation. *Trends Cell Biol*. **20**, 445-452.
Smith, A. B., Pisani, D., Mackenzie-Dodds, J. A., Stockley, B., Webster, B. L. and Littlewood, D. T. J. (2006). Testing the molecular clock: molecular and paleontological estimates of divergence times in the Echinoidea (Echinodermata). *Mol. Biol. Evol*. **23**, 1832-1851.
Sparling, M. L. and Kruszewska, B. (1990). Membrane fractions display different lipid and enzyme content in three cell types in 16-cell stage embryos of sea urchins. *Biochim. Biophys. Acta* **1028**, 117-140.

Spiro, D. J., Boll, W., Kirchhausen, T. and Wessling-Resnick, M. (1996). Wortmannin alters the transferrin receptor endocytic pathway in vivo and in vitro. *Mol. Biol. Cell* **7**, 355-367.
Tanaka, S. and Dan, K. (1990). Study of the lineage and cell cycle of small micromeres in embryos of the sea urchin, *Hemicentrotus pulcherrimus*. *Dev. Growth Differ.* **32**, 145-156.
Thorpe, J. L., Doitsidou, M., Ho, S.-Y., Raz, E. and Farber, S. A. (2004). Germ cell migration in zebrafish is dependent on HMGCoA reductase activity and prenylation. *Dev. Cell* **6**, 295-302.
Uchida, N., Dykstra, B., Lyons, K., Leung, F., Kristiansen, M. and Eaves, C. (2004). ABC transporter activities of murine hematopoietic stem cells vary according to their developmental and activation status. *Blood* **103**, 4487-4495.
Voronina, E., Lopez, M., Juliano, C., Gustafson, E., Song, J., Extavour, C., George, S., Oliveri, P., McClay, D. and Wessel, G. (2008). Vasa protein expression is restricted to the small micromeres of the sea urchin, but is inducible in other lineages early in development. *Dev. Biol.* **314**, 276-286.
Wessel, G. M. and Vacquier, V. D. (2004). Isolation of organelles and components from sea urchin eggs and embryos. *Methods Cell Biol.* **74**, 491-522.
Whalley, T., Terasaki, M., Cho, M. and Vogel, S. (1995). Direct membrane retrieval into large vesicles after exocytosis in sea-urchin eggs. *J. Cell Biol.* **131**, 1183-1192.
Wu, C. T., Budding, M., Griffin, M. S. and Croop, J. M. (1991). Isolation and characterization of *Drosophila* multidrug resistance gene homologs. *Mol. Cell. Biol.* **11**, 3940-3948.
Yabe, T., Suzuki, N., Furukawa, T., Ishihara, T. and Katsura, I. (2005). Multidrug resistance-associated protein MRP-1 regulates dauer diapause by its export activity in Caenorhabditis elegans. *Development* **132**, 3197-3207.
Yajima, M. and Wessel, G. M. (2010). Small micromeres contribute to the germline in the sea urchin. *Development* **138**, 237-243.
Zhou, S., Morris, J. J., Barnes, Y., Lan, L., Schuetz, J. D. and Sorrentino, B. P. (2002). Bcrp1 gene expression is required for normal numbers of side population stem cells in mice, and confers relative protection to mitoxantrone in hematopoietic cells in vivo. *Proc. Natl. Acad. Sci. USA* **99**, 12339-12344.
Zhou, S.-F., Wang, L.-L., Di, Y. M., Xue, C. C., Duan, W., Li, C. G. and Li, Y. (2008). Substrates and inhibitors of human multidrug resistance associated proteins and the implications in drug development. *Curr. Med. Chem.* **15**, 1981-2039.

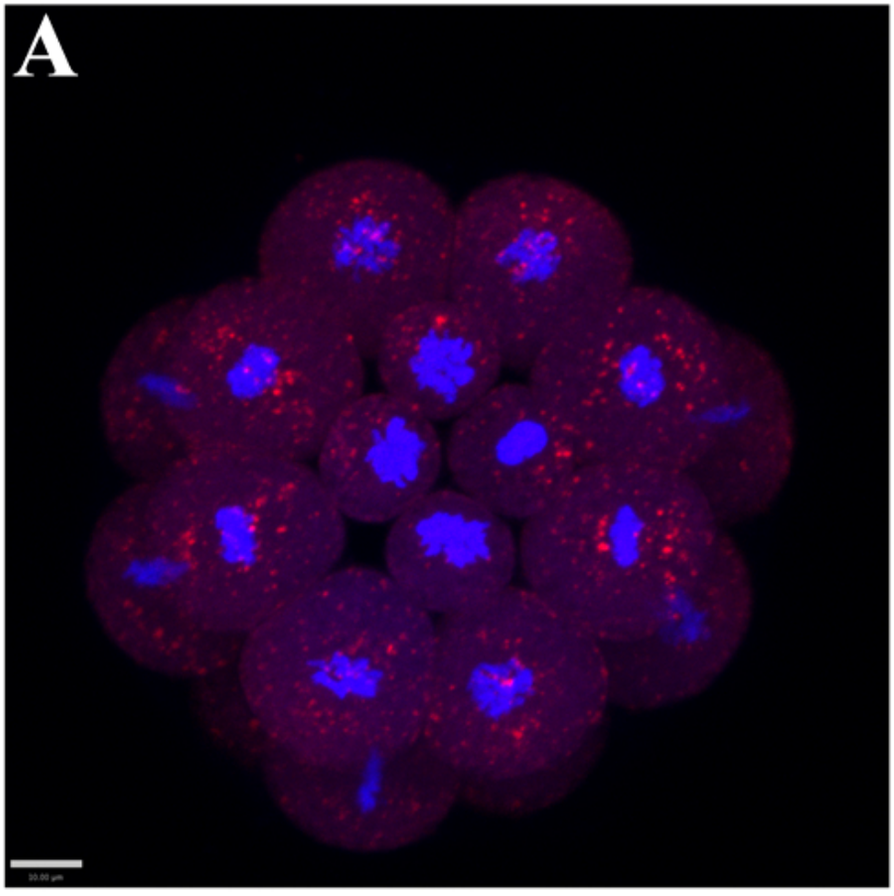
A

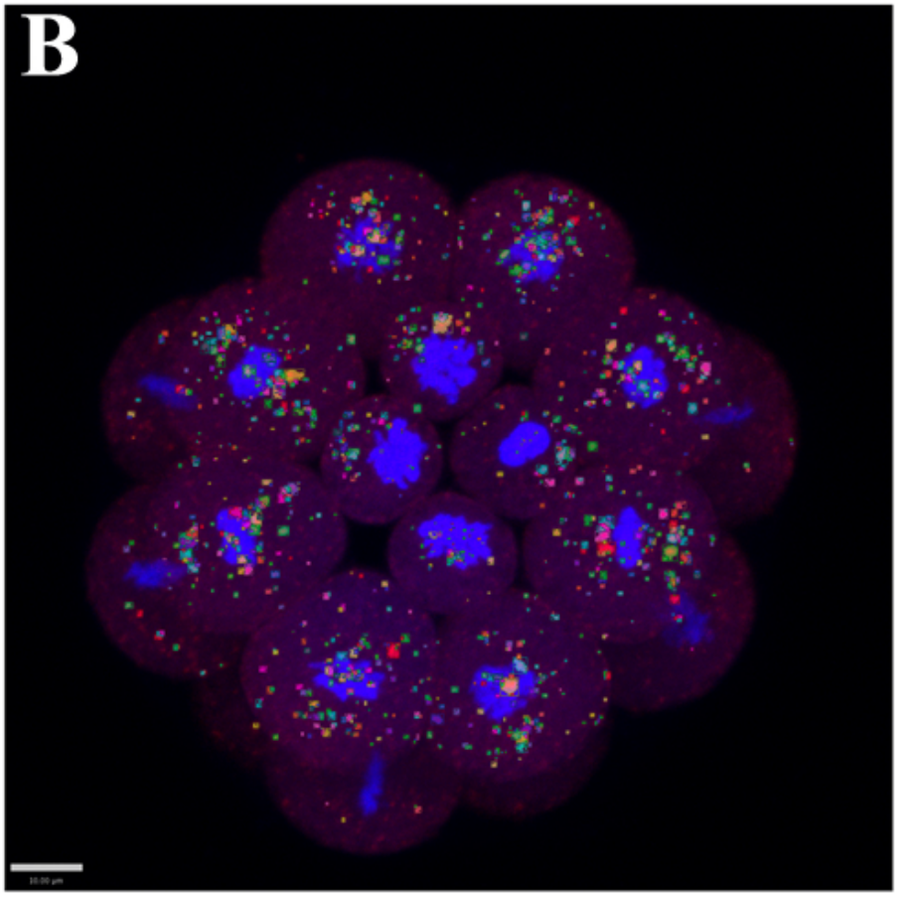
B

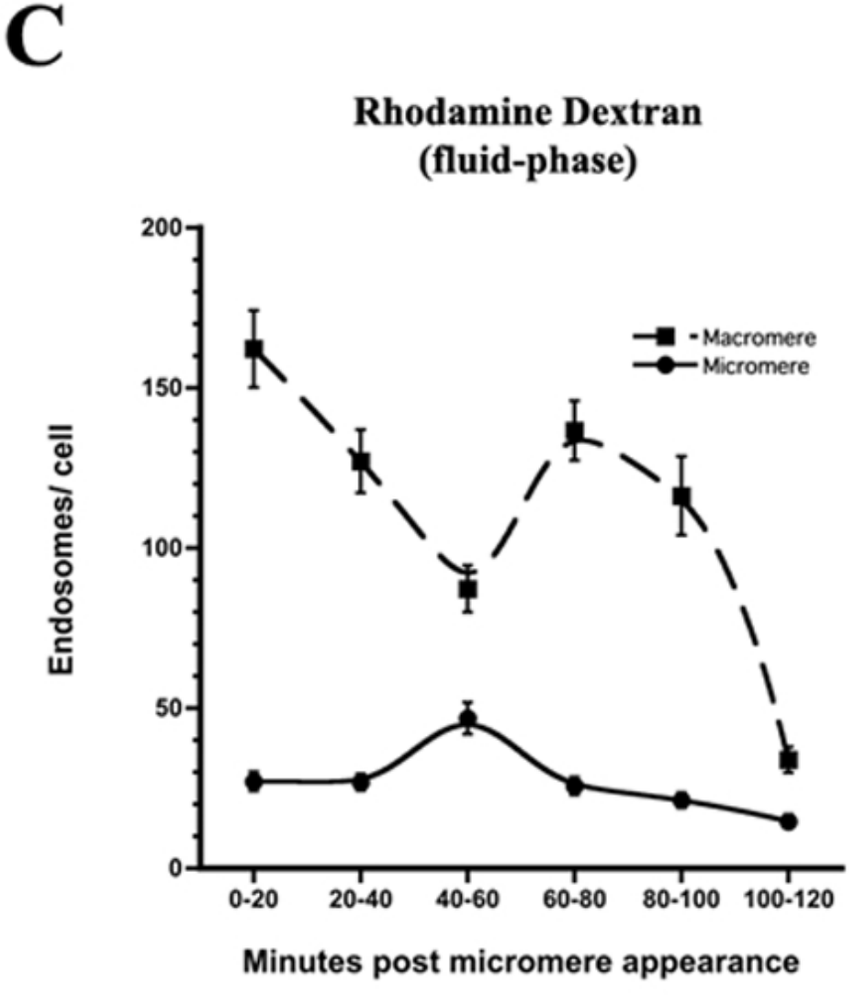
C
Rhodamine Dextran
(fluid-phase)
Macromere
Micromere
Endosomes/ cell
200
150
100
50
0
0-20
20-40
40-60
60-80
80-100
100-120
Minutes post micromere appearance

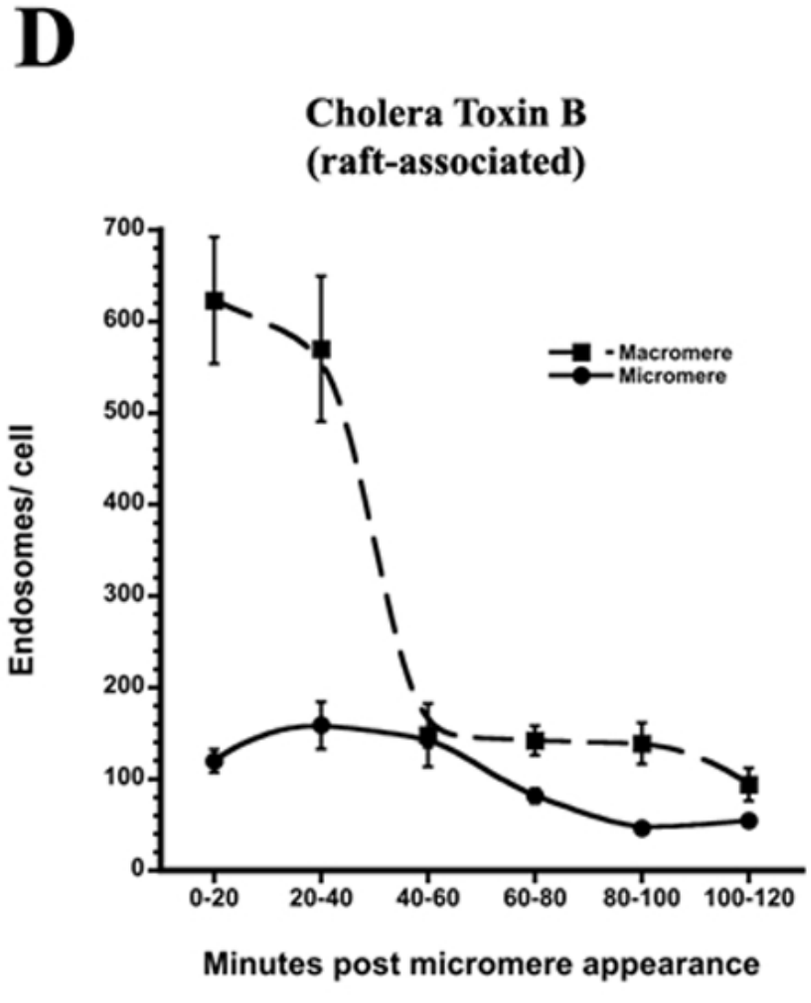
D
Cholera Toxin B
(raft-associated)
Macromere
Micromere
Endosomes/ cell
700
600
500
400
300
200
100
0
0-20
20-40
40-60
60-80
80-100
100-120
Minutes post micromere appearance

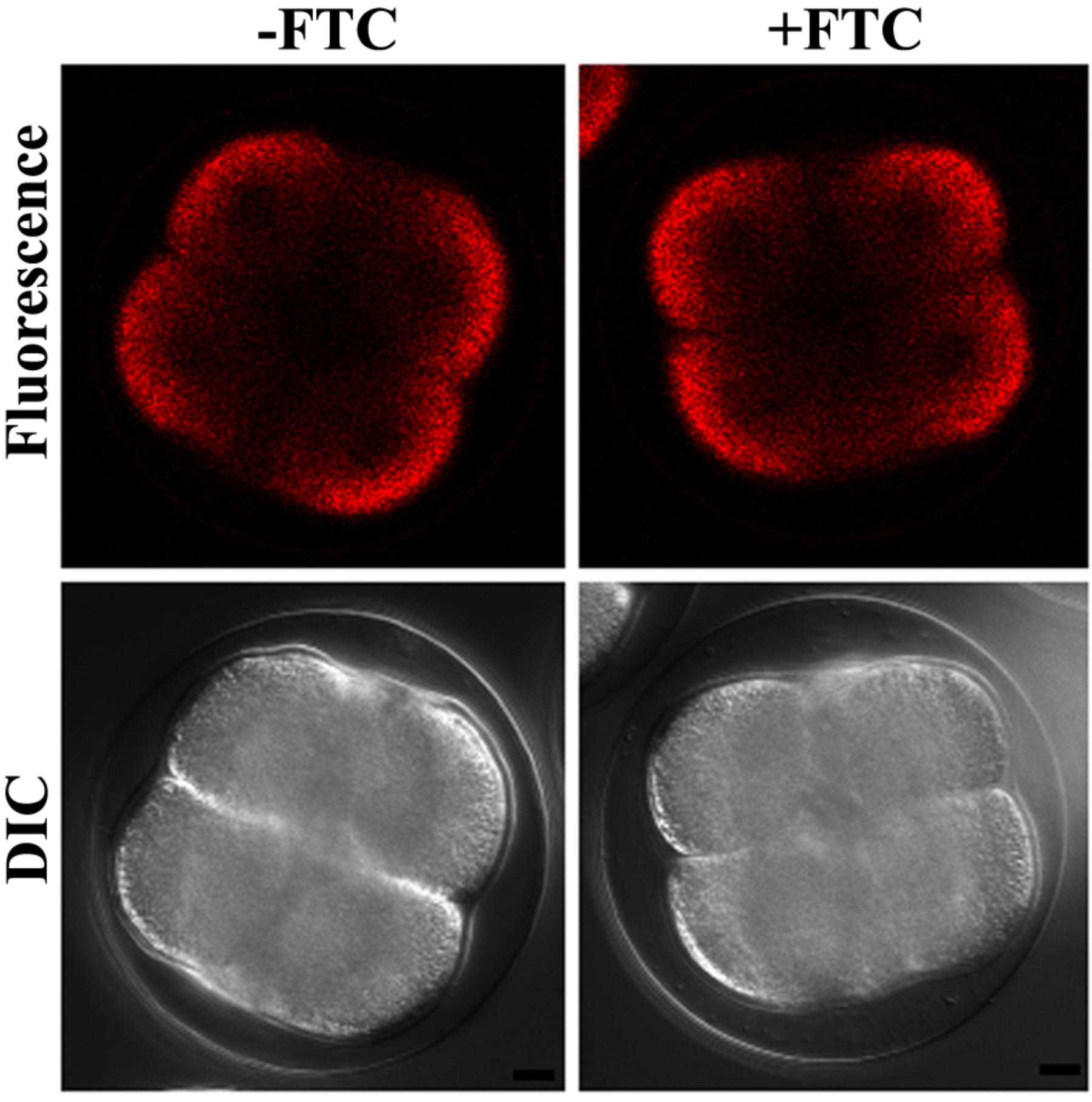
-FTC
+FTC
Fluorescence
DIC